Mini-Review

Myocardial flow reserve (MFR) with positron emission tomography (PET)/computed tomography (CT): clinical impact in diagnosis and prognosis

Maria Cecilia Ziadi

Non-Invasive Cardiovascular Imaging Department, Diagnóstico Médico Oroño, Rosario, Santa Fe, Argentina

Correspondence to: Dr. Maria Cecilia Ziadi, MD. Non-Invasive Cardiovascular Imaging Department, Diagnóstico Médico Oroño, 1515 Oroño Boulevard, Rosario, Santa Fe, S2000DTC, Argentina. Email: mcziadi@hotmail.com.

Abstract: In recent years, radionuclide myocardial perfusion imaging (MPI) using positron emission tomography/computed tomography (PET/CT) has emerged as a robust tool for the diagnosis, risk stratification and management of patients with known or established coronary artery disease (CAD). Cardiac PET/CT imaging affords key advantages compared to single photon emission computed tomography (SPECT) that encompass: (I) improved diagnostic accuracy; (II) decreased radiation exposure due to the utilization of short-lived radiopharmaceuticals, and importantly; (III) the ability to quantify noninvasively myocardial blood flow (MBF) in absolute terms, that is in ml per minute per gram of tissue. Quantitative approaches that measure MBF with PET can facilitate the diagnosis of multivessel CAD and offer the opportunity to monitor responses to lifestyle and/or risk factor modification and to therapeutic interventions. The aim of this review is to focus on the potential clinical utility of MBF and will discuss: (I) basics aspects of PET clinical perfusion tracers and flow quantification parameters; (II) limitations of relative MPI, (III) summarize a classification of diseases where flow quantification may be of use; (IV) specifically, review data on the diagnosis and prognostic value of flow quantification.

Keywords: Positron emission tomography/computed tomography (PET/CT); myocardial flow reserve; clinical value

Submitted Feb 09, 2017. Accepted for publication Apr 11, 2017.
doi: 10.21037/cdt.2017.04.10
View this article at: http://dx.doi.org/10.21037/cdt.2017.04.10

General principles of PET imaging

PET imaging is based on the use of radiotracers that decay by positron emission. A positron, which is a positively charged electron, is emitted from the nuclei of unstable isotopes during radioactive decay. The ejected positron is successively slowed down by Coulomb interaction with numerous nearby electrons. Then, both the positron and an electron undergo a process known as positron annihilation and are converted into two coincident gamma-ray photons of 511 keV that travel at opposite directions with an angle close to 180 degrees apart from each other (1). Electronic detectors are placed on either side of the active volume and connected in a coincidence circuit. When many such events are detected, the activity distribution of the positron-emitting radionuclide within a volume of interest may be reconstructed. The electronic detection of these photons in coincidence constitutes the foundation of PET imaging (2).

PET vs. SPECT

Cardiac imaging using PET provides several technical advantages over the conventional SPECT and is described as follows: (I) accurate depth-independent attenuation correction (AC) decreases the number of false-positives and as a result, augments specificity. Besides, AC makes it

Table 1 Myocardial PET flow tracers

Pharmaceutical	Radioisotope	Physical half-life	Production method	Parent compound physical half-life	Physiology	Primary application	Average positron energy (MeV)	RMS positron range (mm)
Water	O-15	122 s	Cyclotron	–	Diffusible	Perfusion	0.74	1.02
Ammonia	N-13	10 min	Cyclotron	–	Diffusible/retained	Perfusion	0.49	0.57
Rubidium	Rb-82	76 s	^{82}Sr/^{82}Rb generator	^{82}Sr=25.5 days	Extracted/retained	Perfusion	1.48	2.60

possible absolute MBF quantification. (II) higher spatial resolution improves the detection of small perfusion defects, and thus, increases sensitivity. (III) superior temporal resolution (5–10 s) permits fast dynamic imaging of tracer kinetics and makes absolute quantification of myocardial perfusion possible. (IV) higher extraction fractions and shorter half-lives of the commonly used radiotracers (^{82}Rubidium or ^{13}N-ammonia) in comparison with SPECT agents [technetium-99m (^{99m}Tc)-sestamibi, thallium-201 (^{201}Tl)], would permit detection of lesser degrees of ischemia as well as faster assessment of myocardial perfusion, respectively. (V) Although stress perfusion abnormalities can be identified with conventional SPECT in the majority cases, the interpretation of PET perfusion images is less equivocal, possibly due to the better quality images. Furthermore, ECG-gated PET is able to assess left ventricular (LV) function at rest and during peak stress (as opposed to post stress with gated SPECT) (2-5).

Clinical PET perfusion tracers

MBF PET tracers that are current Food and Drug Administration (FDA) approved and Centers for Medicare and Medicaid services (CMS)-reimbursable PET MBF tracers are limited to ^{82}Rb and ^{13}N-ammonia. While ^{15}Oxygen-water ($H_2{}^{15}O$)—a freely diffusible tracer—is also used clinically in Europe, it is not FDA approved in the United States (6) (see *Table 1*). There are also ^{18}F-labeled MBF agents that are currently investigational and in clinical trials.

Nitrogen-13 Ammonia ($^{13}NH_3$)

Its physical half live of 10 min. requires an onsite cyclotron and radiochemistry synthesis capability (7,8). The extraction fraction is approximately 80% in the resting state, but like other no diffusible tracers it decreases as MBF increases (*Figure 1*).

In patients with severe impairment of the left ventricular ejection fraction (LVEF), chronic obstructive pulmonary disease (COPD) and smoking, the sequestration of $^{13}NH_3$ in the lungs can be abnormally increased (9).

Rubidium-82 (^{82}Rb)

^{82}Rb is produced from a strontium-82 (^{82}Sr)/^{82}Rb generator and it is widely available in the US, with increasing availability in Canada, and in several regions of Europe and Japan. It has a short physical half-life of 76 s. Furthermore, patient and staff radiation exposure is significantly reduced compared to conventional technetium-99m (^{99m}Tc) SPECT because of the much shorter scan time and no waiting time to clear background radiation (2). ^{82}Rb is a monovalent cationic analogue of potassium and has similar biological activity to ^{201}Tl. Myocardial uptake of ^{82}Rb requires active transport via the sodium/potassium adenosine triphosphate transporter, which is dependent on coronary blood flow. There is accurate data available in the literature with ^{82}Rb MPI linked to outcomes (10-12).

Novel ^{18}F-labeled agents for PET myocardial perfusion imaging

^{18}F-tagged agents can take the full advantage of PET superior spatial resolution. Flurpiridaz is an inhibitor of mitochondrial complex I (MC-1), with a physical half-life of 110 minutes, has a high first-pass extraction with less roll-off. Flurpiridaz has demonstrated an excellent relationship to flow in animal models (and in humans has shown a very good diagnostic accuracy for the detection of significant CAD (13,14). Regarding its potential for quantification of absolute MBF, in an experimental study, measurement of the standardized uptake value (SUV) obtained at 5 to 10 minutes after ^{18}F-flurpiridaz IV injection showed a linear

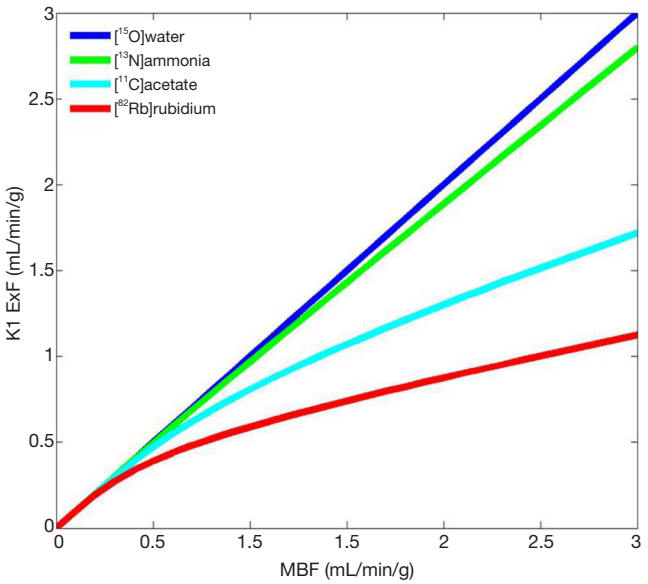

Figure 1 Tracer uptake rate K_1 *vs.* FLOW from a one-tissue-compartment model of tracer kinetics. K_1 is equal to the product of FLOW times the unidirectional extraction fraction. In all tracers except ^{15}O-water, the tracer extraction is reduced when perfusion is increased leading to underestimation of perfusion if only tracer uptake is used.

correlation with adenosine hyperemia MBF as quantified by radiolabeled microspheres. This tracer is currently in phase III clinical trials.

Why MBF quantification with PET/CT?

Although other modern imaging techniques are currently being investigated, PET remains the most accurate noninvasive modality for MBF quantification and the modality to which others are compared. Its accuracy has been extensively validated in experimental animals and humans, and the reproducibility of this technique is well established (15-17). However, multiple factors have limited widespread clinical application including availability of scanners, increased cost, and reimbursement issues.

Quantification of MBF using PET has been broadly applied in research for many years. Nowadays, PET measurements of MBF and MFR yield a paradigm shift in the evaluation and management of patients with CAD. In light of the recent shift in the management of CAD from an anatomical gold standard (i.e., coronary angiogram) to a functional one, PET MBF quantification may enable definition of the entire spectrum of vascular dysfunction: from endothelial dysfunction related cardiovascular risk factors or early atherosclerosis and non-coronary cardiac diseases; to advanced diffuse atherosclerotic disease. Various research studies have suggested an incremental prognostic value of MBF assessed with PET imaging in CAD and other cardiac conditions (18-22). As previously mentioned the use of hybrid imaging enables functional and anatomical data, namely, the unique opportunity to visualize and characterize the atherosclerotic burden, coronary stenosis and evaluate the functional consequences of a specific anatomic lesion in a single step (23) (*Figure 2*). It is important to mention that visualization of the coronary arteries requires administration of an intravenous iodinated contrast agent. PET MBF quantification can also serve as a guide to monitor a number of pharmacologic interventions.

MFR can be done with the PET acquisition protocols that are currently utilized (i.e., List Mode Acquisition) without the need of adding time, radiation exposure to the patient and/or additional cost. In order to obtain accurate MBF values, image-derived time-activity curves of the flow tracer from arterial blood and myocardial tissue regions are used as inputs into a validated tracer kinetic model (*Figure 3*) (6). Automated image analysis tools have been used to facilitate relatively robust quantification of MBF and MFR, even accounting for variations across different modeling approaches (24-26).

Hybrid scanners with both coronary anatomical and hemodynamic measurement capabilities are advantageous alternatives with a high diagnostic accuracy, compared to dedicated PET scanners alone (27,28). CT-based attenuation correction and tissue boundary are more effective than traditional radionuclide transmission sources used in dedicated PET. Perfusion abnormalities can be based on the CT-derived anatomy without the use of frequently inaccurate standard assumptions about vascular distribution pattern (27). In addition, hybrid PET/CT allows routine evaluation of relative myocardial perfusion, LV performance at rest and during peak stress, quantification of perfusion and, depending on the CT scanner capabilities, the addition of calcium score estimation and non-invasive evaluation of the epicardial coronary arteries, thus enhancing test sensitivity for diagnosis of CAD. In order to translate PET flow quantification as a routine clinical tool, the method should be proved to be reproducible and validated in animal models and in humans; the tracer and technology should be available, easy to apply

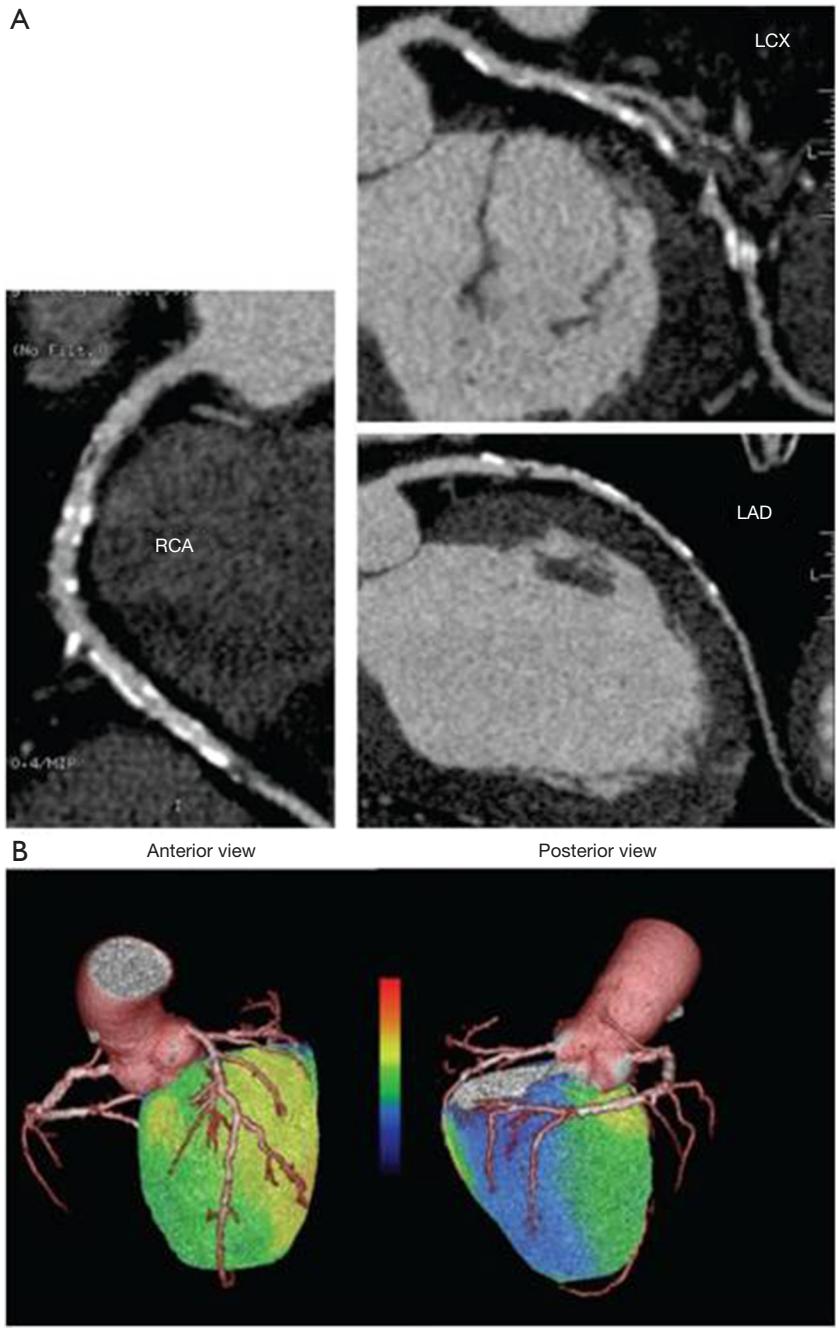

Figure 2 Hybrid PET/CT allows non-invasive evaluation of the coronary anatomy and functional information in one setting. (A) CT angiography (step and-shoot mode) shows multi-vessel disease with massive coronary calcifications and severe stenosis in all major coronary arteries. (B) Hybrid display during adenosine stress demonstrates quite preserved perfusion in anterolateral wall but moderate reduction in septal wall (anterior view). In RCA related region the perfusion was the most severely reduced (posterior view) indicating culprit stenosis in this vessel. Perfusion was colour scaled so that red colour denotes to 3.5 mL/min/g. Resting perfusion was normal (not shown). Total radiation dose of the hybrid study was 11.3 mSv. Reproduced with permission of (21).

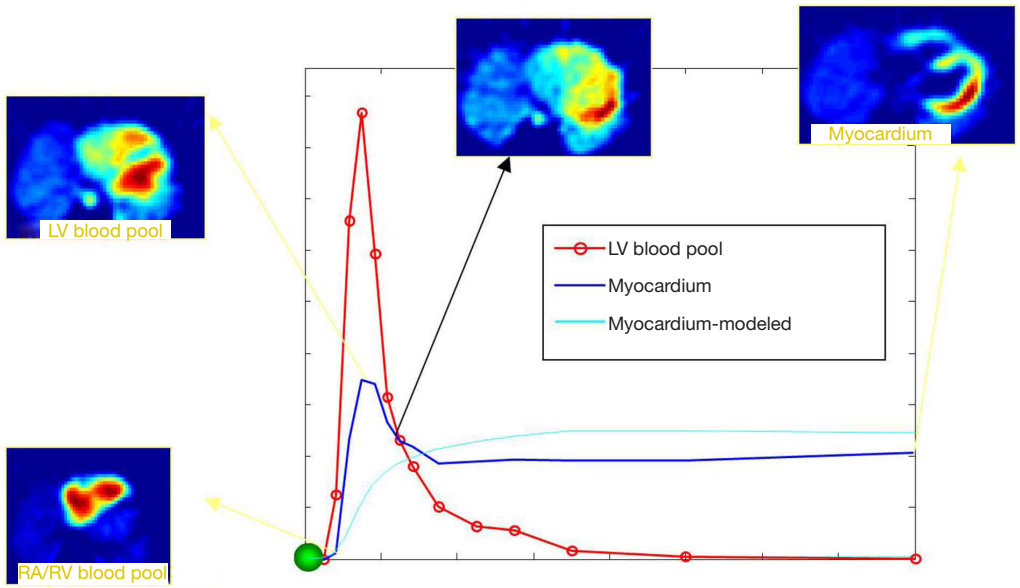

Figure 3 Schematic diagram of Time-Activity curves of tracer radioactivity in Blood and in the myocardium. Flow quantification with PET requires IV injection of a PET perfusion tracer and dynamic acquisition of images. Tracer-kinetic models (1 to 3 compartments) and operational equations are then applied to correct for physical decay of the radioisotope, partial volume-related underestimation of the true myocardial tissue concentrations (by assuming a uniform myocardial wall thickness of 1 cm), and spillover of radioactivity between the left ventricular blood pool and myocardium. Time activity curves, in red in the blood and in light blue the pure tracer concentration after we correct for partial volume and spillover of blood in the myocardium.

into clinical practice, and importantly, demonstrate an added value for diagnostic or prognostic application and/or impact on therapy decision and patient outcomes (29). Over the past 8 years, several observational research studies have been published in regards of the potential value of MFR in the clinical setting, particularly in patients with known or suspected CAD. Indeed the recently published ASNC PET guidelines (6) have incorporated and enumerate some clinical potential applications of this tool.

MBF PET parameters

Resting MBF is the absolute amount of blood flow that the myocardium receives per minute per gram of tissue under baseline conditions. It is affected by several factors, including age, gender, hemoglobin content, heart rate, blood pressure, drugs, myocardial contractility and cardiac work which can be estimated by the rate pressure product (RPP) (30). In normal individuals, average values of MBF at rest are 0.6 to 1.3 mL/min/g (average, 0.98±0.23 mL/min/g) (30,31). There is a linear association between resting MBF and age (32), which is partly explained by the trend for an association between age and RPP (33).

Hyperemic blood flow (or stress flow) represents the maximum blood flow that can be supplied to the heart during maximum vasodilatation of the coronary vascular bed. Usually, this is achieved by intravenous pharmacologic agents, such as vasodilators or inotropic agents (6). Factors that affect measurement of stress MBF include: caffeine and its derivatives, increased microvascular tone, anatomic remodeling of the microcirculation, submaximal coronary vasodilatation, increased extravascular resistance, coronary risk factors, autonomic nervous system dysfunction and systemic inflammation (34). PET MBF quantification is not possible with treadmill testing because the early time frames post-tracer injection cannot be acquired. Cold pressor test (CPT) and mental stress test have been applied in the research laboratory to induce hyperemic MBF. CPT provokes a mixed vascular response with adrenergically mediated vasoconstrictor and vasodilatory response, reflecting mostly endothelium-dependent vasodilatation.

Myocardial flow reserve (MFR) constitutes the ratio of MBF during maximal coronary vasodilatation to resting MBF and is therefore impacted by both rest and stress

flow. MFR represents the relative reserve of the coronary circulation. The optimal cut-point between normal and abnormal has been somewhat empirical and there is some variability in the literature in part depending on the flow tracer applied and on different software, but at general it is accepted that MFR values can be interpreted as follows:

(I) MFR more than 2.3 indicates a favorable prognosis (assuming that there is no lower regional value).
(II) MFR less than 1.5 suggests significantly diminished flow reserve (in the absence of concomitant elevated resting blood flow), and is associated with elevated cardiac risk.

According to the recently published ASNC guidelines (6), MFR with PET appear most helpful in:

- Patients without known prior history of cardiac disease who present with symptoms suspicious for myocardial ischemia;
- Patients with known CAD, in whom more specific physiological assessment is desired;
- Identifying an increased suspicion for multivessel CAD;
- Situations with a disparity between visual perfusion abnormalities and apparently normal coronary angiography, in order to assess possible microvascular dysfunction;
- Heart transplant when there is a question of vasculopathy.

Role of MBF quantification to optimize detection of microvascular disease

Although the diagnosis of CAD has been traditionally focused on obstructive atherosclerosis of the epicardial arteries, in recent years significant focus has turned to abnormalities of function and structure that reside at the level of the microcirculation (small vessels; 300–400 μm)—so-called microvascular dysfunction. Evaluation of the coronary microcirculation *in vivo* relies on the measurement of parameters that are indices of its functional status, such as absolute MBF and MFR (34). In the absence of epicardial CAD, impaired MFR may reflect changes associated with cardiovascular risk factors (35-38), such as hypercholesterolemia, hypertension, diabetes mellitus (DM), and smoking, (all known to have a deleterious effect on the vessel wall). The WISE study (39) has shown that women with ischemic heart disease symptoms, but without significant coronary artery stenosis were at higher risk of cardiovascular events than women without any symptoms, most likely due to endothelial dysfunction. MFR determined using PET has also been used as a surrogate end point to assess efficacy of treatments aimed at halting or delaying the progression of the atherosclerotic process.

Role of MBF quantification in established coronary artery disease

Since the pioneering studies performed by Gould *et al.* in the late 70s (40,41), MFR has been proposed as an functional indicator of the severity of CAD. MBF at rest remains normal during the progression of coronary lesions until there is an 80–85% diameter stenosis, while hyperemic MBF measured after maximal vasodilatation begins to decrease progressively if the stenosis is more than about 40% (41). Uren *et al.* showed the relationship between coronary artery stenosis on angiography and MFR data obtained by $H_2{}^{15}O$ PET (42). Similar results were obtained with $^{13}NH_3$ (43). Di Carli *et al.* showed that intermediate severity coronary lesions exhibited a differential MFR that decreased with increasing stenosis severity (44).

A well-known limitation of relative MPI with both PET and SPECT is that this method often uncovers only coronary territories supplied by coronary arteries with the most severe stenosis, and therefore, it is relatively insensitive to accurately delineate the extent of obstructive angiographic CAD in patients with balanced ischemia due to multivessel CAD (45-47). These observations have served as the basis for the clinical use of quantitative MBF may help overcome these limitations and to improve identifications of obstructive CAD, particularly to exclude the presence of multivessel CAD. Parkash *et al.* (46) illustrated sensitivity of semi-quantitative and quantitative ^{82}Rb PET nearly on par (87% *vs.* 83%), but correct identification of disease in all three diseased vascular territories (≥70% stenosis in each territory) was significantly better with quantitative ^{82}Rb PET (46% *vs.* 92%). In a more recent study (47), we enrolled 120 patients with known or suspected CAD, and demonstrated that patients with 3-vessel CAD had a significantly lower MFR compared to patients without (*Figure 4*). Global MFR (<2.0) was concluded as an independent predictor of 3-vessel CAD, by results from a multivariable Cox analysis including summed stress score (SSS), MFR, and other significant risk factors. MFR had a diagnostic sensitivity of 88% for 3-vessel disease, whereas only 60% of these patients had other generally accepted risk

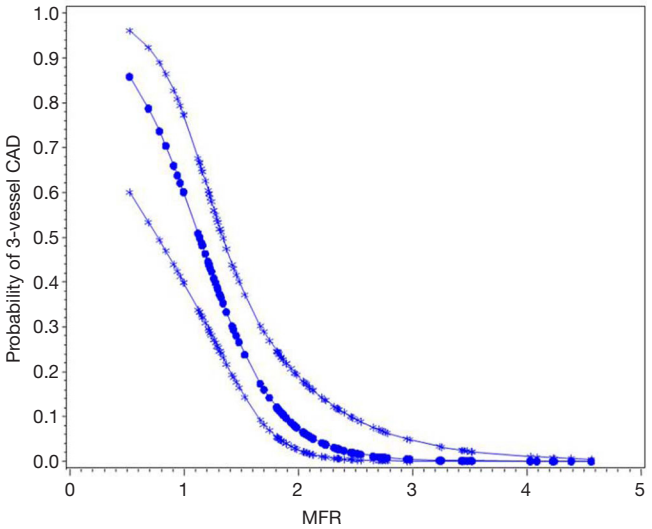

Figure 4 Unadjusted predicted probability (red line) and 95% Confidence Interval (blue lines) of severe 3 vessel CAD at various levels of ^{82}Rb PET MFR based on the analysis model. When MFR is preserved, the likelihood of multivessel CAD is low, whereas with reducing MFR the likelihood of 3-vessel CAD increases. MFR, myocardial flow reserve. Reproduced with permission of (47).

factors, such as reduced ejection fraction, transient ischemic dilation, and ischemic ECG changes. *Figures 5,6* illustrate case examples. In line with previous results, another study showed that a global preserved MFR (>2.0) provides a high negative predictive value of 97% to exclude the presence of 3-vessel CAD, regardless of relative perfusion results (48).

From the information provided it is apparent that MFR represents a sensitive parameter, but not necessarily specific for obstructive epicardial CAD. In several patients with overt CAD and reduced global, microvascular disease together with epicardial stenosis coexists, and thus the ability of separating these two when regional perfusion defects are missing, is difficult. As stated earlier, in this regard, the information provided by CT angiography (CTA) in hybrid scanners PET/CT can facilitate the diagnosis or exclusion of epicardial coronary stenosis (23,49-51). With exclusion of stenosis, functional information with decreased MFR will point to microvascular dysfunction and subclinical CAD.

Role of MBF quantification in non-CAD microvascular diseases

In patients with hypertrophic cardiomyopathy (HCM), symptoms and signs of myocardial ischemia are usually present. In the absence of significant coronary stenosis, this finding is indicative of diffuse microvascular dysfunction. It appears that besides reduced capillary density caused by hypertrophy, extravascular compressive forces contribute to endothelial dysfunction (52), and that inadequate hyperemic MBF response to demand in patients with HCM predisposes to myocardial ischemia. Cecchi *et al.* (21) showed that altered microvascular function is strongly associated with poor outcomes. In line with these observations, Olivotto *et al.* (20) suggested that the degree of microvascular dysfunction is a potent long term predictor of remodelling and systolic impairment, while a preserved vasodilator capacity was associated with a powerful protective effect.

Among patients with idiopathic dilated cardiomyopathy (IDCM), impaired MBF at rest and during hyperemia with reduced MFR have been demonstrated in PET research studies (19,53). Neglia *et al.* (18) reported that global impaired vasodilator capacity is an independent predictor of subsequent cardiac events and associated with an increased risk of death and further progression of CHF.

These findings have enhanced our understanding of the role of microvascular dysfunction in these cardiac conditions. However, it is not clear how PET flow measurements will be helpful to: (I) diagnose these conditions—keeping in mind that MFR is affected by many factors and thus may be rather nonspecific; (II) monitor disease progression; and (III) direct management decisions towards strategies that impact outcomes. Continued research is needed to clearly ascertain this clinical role of PET flow quantification (29).

Clinical added prognostic value of MBF quantification

Quantitative myocardial perfusion constitutes a valuable tool for risk stratification both in CAD states and in other clinical conditions, as previously described. MFR provides higher sensitivity to uncover the total burden of myocardial ischemia and overall vascular health that has shown to be reproducible data in several research studies.

In a prospective cohort study with 704 consecutive patients assessed for ischemia, we found that patients with abnormal MFR (<2.0) had a significantly higher cardiac event rate after one year of follow-up (54). MFR was the strongest predictor of MACE with the highest hazard ratio. Importantly, an abnormal MFR identified patients at

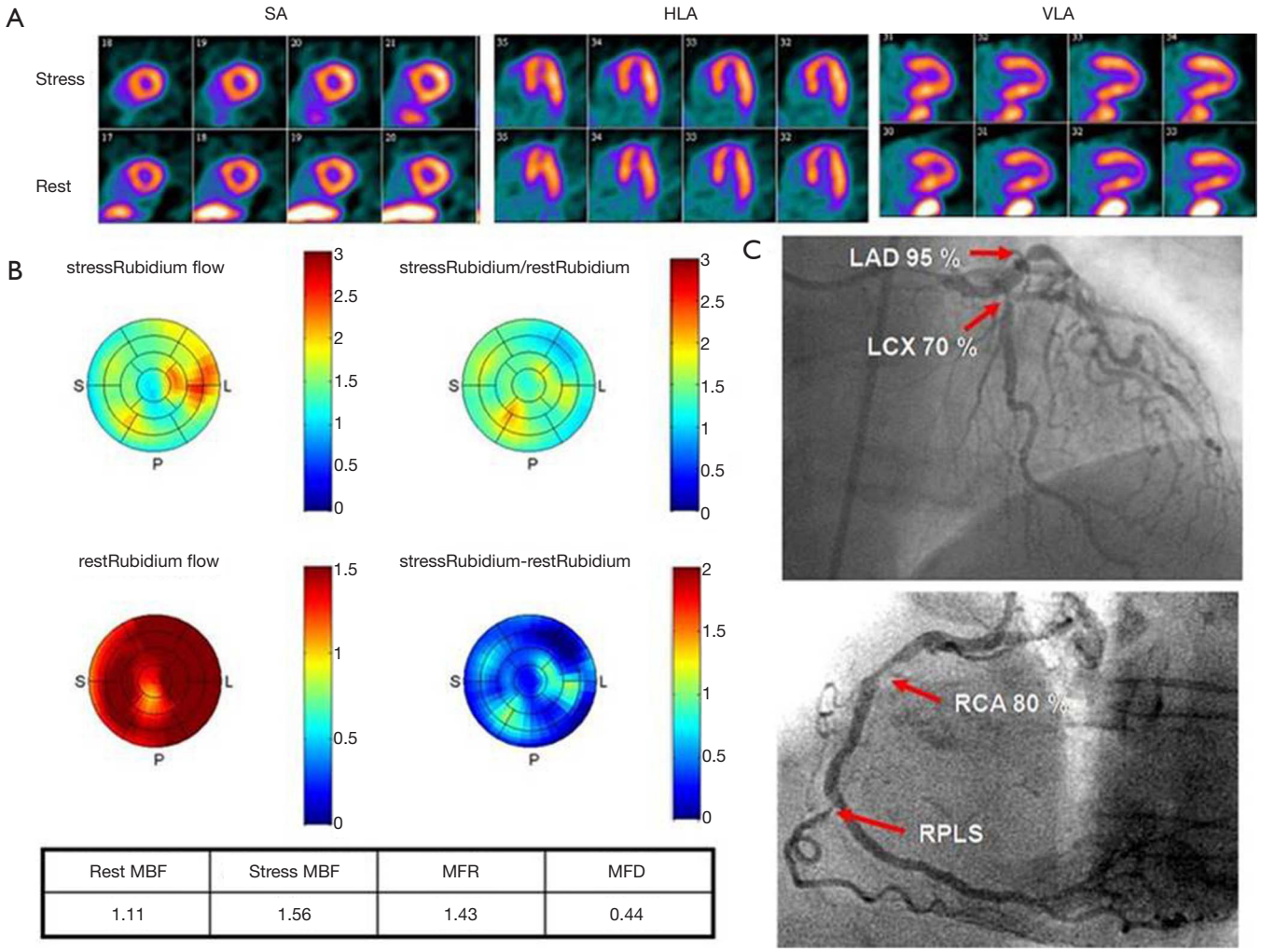

Rest MBF	Stress MBF	MFR	MFD
1.11	1.56	1.43	0.44

Figure 5 Clinical example in which flow quantification with PET may improve diagnosis of CAD. (A) Dypiridamole ^{82}Rb PET MPI static images demonstrate normal relative perfusion at rest and during peak stress; (B) 17-segment model polar maps of rest MBF (lower left; color display scale 0 to 1.5 mL/min/g), stress MBF (upper left; scale: 0–3.0 mL/min/g), MFR (upper right; scale: 0–3.0) and MFD (lower right; scale: 0–2.0) which demonstrate global impairments, absolute values displayed in the table below; (C) Coronary Angiogram reveals significant obstructive 3-vessel CAD, relative perfusion underestimated the presence of disease (arrows point out significant stenosis). HLA, horizontal long axis; SA, short axis; VLA, vertical long axis; MBF, myocardial blood flow; MFR, myocardial flow reserve; MFD, myocardial flow difference; LAD, left anterior descending artery; LCX, left circumflex; RCA, right coronary artery; RPLS, right posterolateral branch.

increased risk of cardiac death even among those normal scans by semi-quantitative visual analysis (*Figure* 7). These results were extended by two other prognostic studies with slightly smaller enrolled populations, that is, n=275 and n=351, of patients referred for known or suspected CAD (55,56). The semi-quantitative measurements had a significant prognostic value in all three studies as well. Recently, a large study including 2,783 consecutive patients referred for known or suspected CAD, documented global MFR's incremental value for prognostication over other recognized clinical risk factors, including LV systolic function and a semi-quantitative assessment of myocardial ischemia. Patients in the lowest tertile of MFR (<1.5) had a significantly worse prognosis with a 6-fold increase risk of death that was independent of other risk factors. On the other hand, patients in the highest tertile of MFR (>2.0)

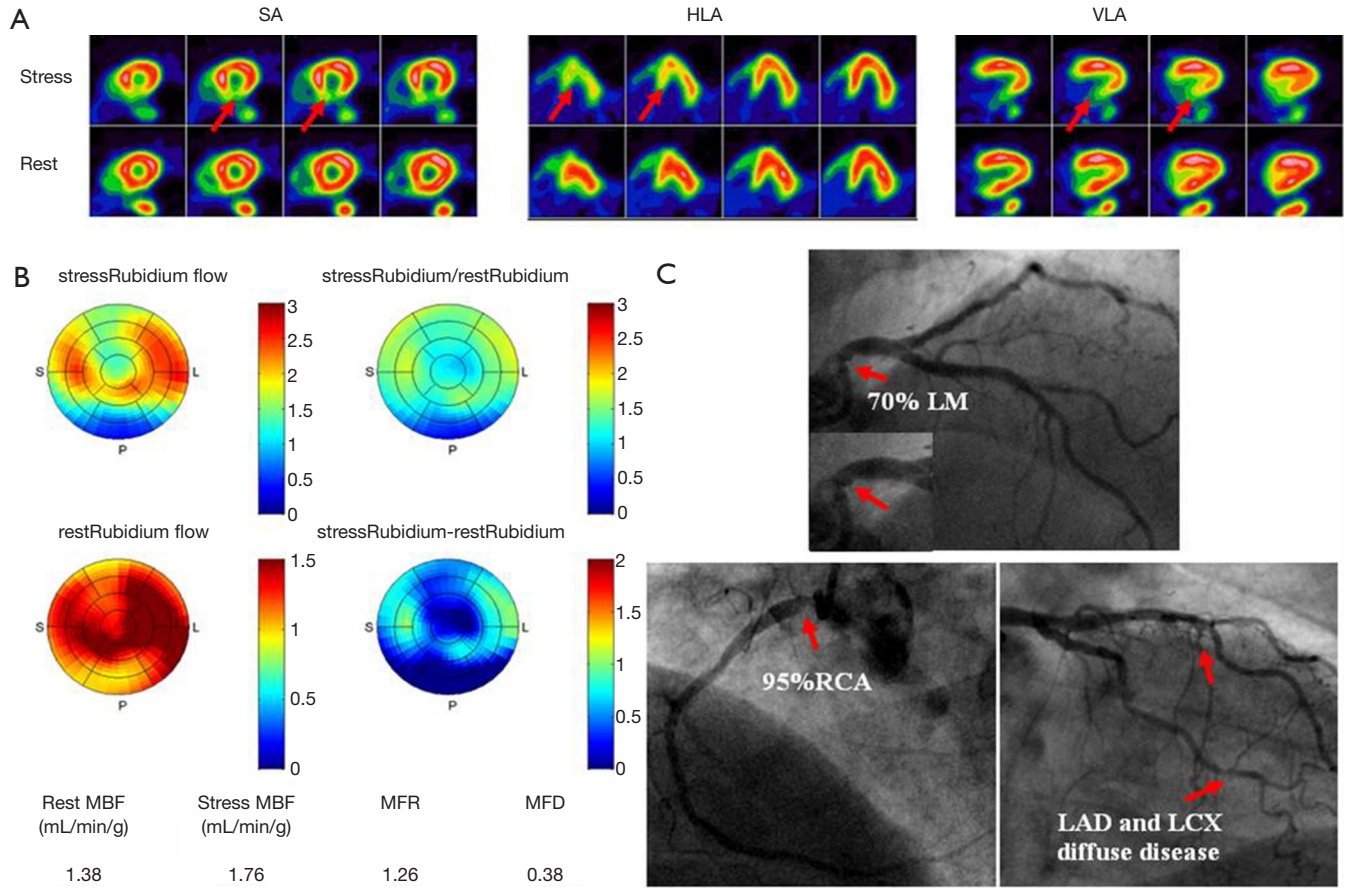

Figure 6 A 70-year-old male with hypertension, PVD, renal insufficiency, worsening angina with exertion. (A) dipyridamole ^{82}Rb PET MPI static images demonstrate moderate ischemia in the RCA territory (red arrows); (B) 17-segment model polar maps of rest flow (lower left; color display scale 0–1.5 mL/min/g), stress flow (upper left; scale: 0–3.0 mL/min/g), MFR (upper right; scale: 0–3.0) and MFD (lower right; scale: 0–2.0) with several global reduction in MFR; (C) coronary anatomy showed severe LM stenosis and critical ostial RCA with diffuse CAD in LAD and LCX (arrows point out significant stenosis). Relative MPI underestimated CAD in LM territory. HLA, horizontal long axis; SA, short axis, VLA, vertical long axis; MBF, myocardial blood flow; MFR, myocardial flow reserve; MFD, myocardial flow difference. Reproduced with permission of (47).

had a good prognosis despite of other risk factors resulting in correct reclassification of risk in a large group of patients, including 35% of intermediate risk patients (57).

The prognostic value of MFR can be also applicable to patients with DM and in patients with chronic renal dysfunction. For patients with DM, an abnormal MFR can predict higher rates of cardiac and all-cause mortality (58). Of note, diabetic patients without known CAD and with impaired MFR experienced a rate of cardiac death comparable to, and possibly higher than, that for nondiabetic patients with known CAD. Likewise, in patients with moderate to severe renal dysfunction (estimated glomerular filtration rate less than 60 mL/min/1.73 m^2) clinically referred for PET MPI, impaired CFR less than 1.5 was associated with an adjusted 2.1-fold increase in the risk of cardiac death (P<0.01) (59).

Concluding remarks and future directions

Cardiac PET and PET/CT are rapidly evolving; MFR with PET represents a sensitive means by which to uncover the presence of CAD, particularly to delineate the extent of disease, also to estimate the functional importance of hemodynamically significant epicardial disease, and

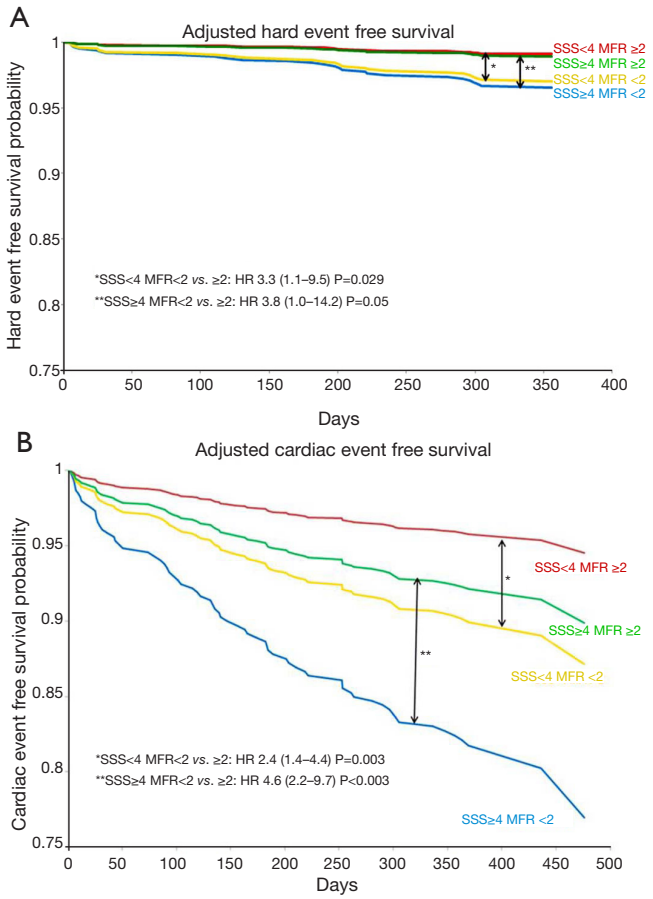

Figure 7 MACE within subgroups of SSS for different levels of MFR. At any level of SSS, the prevalence of MACE is higher in patients with the lowest MFR (<1.5), and statistically significant different compared to MFR ≥2 among patients with overt ischemia. (*P=0.028 for SSS ≥4–7 and MFR <1.5 *vs.* MFR ≥2 and **P=0.002 for SSS ≥8 and MFR <1.5 *vs.* MFR ≥2). SSS, summed stress score; MACE, major adverse cardiac events; MFR, myocardial flow reserve. Reproduced with permission of (55).

improve risk stratification of patients. In spite of the limited specificity of MFR, the capability to separate coexisting ischemic conditions can be quite challenging, and may be supported by the addition of CTA to the PET/CT session, thus, providing complementary useful information.

Estimation of flow quantification with PET and integration with traditional relative MPI is relative straightforward utilizing specific standardized protocols and highly reproducible software algorithms that consecutively, facilitate implementation of MFR in clinical routine. Compelling evidence in the literature supports that quantification of MBF with PET has the power to become a reliable non-invasive imaging tool assisting in diagnosis, treatment, and risk stratification of patients with known or suspected CAD and other specific non-ischemic conditions. Last but not least, large randomized controlled trials that evaluate treatment effect are needed to definitively elucidate the clinical significance of MFR on the final outcome in different patient populations.

Acknowledgements

None.

Footnote

Conflicts of Interest: The author has no conflicts of interest to declare.

References

1. Camici PG. Positron emission tomography and myocardial imaging. Heart 2000;83:475-80.
2. Cecilia ZM, Dekemp RA, Yoshinaga K, et al. Diagnosis and Prognosis in Cardiac Disease using Cardiac PET perfusion imaging. In: Zaret BL, Beller GA. editors. Clinical Nuclear Cardiology, Fourth Edition. Philadelphia: Elsevier, 2015.
3. Di Carli MF, Hachamovitch R. New Technology for Nonoinvasive Evaluation of Coronary Artery Disease. Circulation 2006;115:1464-80.
4. Yoshinaga K. Cardiac Applications. In: Wahl RL, Beanlands SB. editors. Principles and Practice in Positron Emission Tomography. 2nd Edition. Philadelphia: Lippincott Williams and Wilkins, 2008.
5. Bateman TM, Heller GV, McGhie AI, et al. Diagnostic accuracy of rest/stress ECG-gated Rb-82 myocardial perfusion PET: comparison with ECG-gated Tc-99m sestamibi SPECT. J Nucl Cardiol 2006;13:24-33.
6. Dilsizian V, Bacharach SL, Beanlands RS, et al. ASNC imaging guidelines/SNMMI procedure standard for positron emission tomography (PET) nuclear cardiology procedures. J Nucl Cardiol 2016;23:1187-226.
7. Krivokapich J, Huang SC, Phelps ME, et al. Dependence of 13NH3 myocardial extraction and clearance on flow and metabolism. Am J Physiol 1982;242:H536-42.
8. Hutchins GD, Schwaiger M, Rosenspire KC, et al. Noninvasive quantification of regional blood flow in the

human heart using N-13 ammonia and dynamic positron emission tomographic imaging. J Am Coll Cardiol 1990;15:1032-42.
9. Machac J, Bacharach SL, Bateman TM, et al. Positron emission tomography myocardial perfusion and glucose metabolism imaging. J Nucl Cardiol 2006;13:e121-51.
10. Yoshinaga K, Chow BJ, Williams K, et al. What is the prognostic value of myocardial perfusion imaging using rubidium-82 positron emission tomography? J Am Coll Cardiol 2006;48:1029-39.
11. Lertsburapa K, Ahlberg AW, Bateman TM, et al. Independent and incremental prognostic value of left ventricular ejection fraction determined by stress gated Rubidium 82 PET imaging in patients with known or suspected coronary artery disease. Journal of Nuclear Cardiology 2008;15:745-53.
12. Dorbala S, Hachamovitch R, Curillova Z, et al. Incremental prognostic value of gated Rb-82 positron emission tomography myocardial perfusion imaging over clinical variables and rest LVEF. JACC Cardiovasc Imaging 2009;2:846-54.
13. Dilsizian V, Taillefer R. Journey in evolution of nuclear cardiology: will there be another quantum leap with the F-18-labeled myocardial perfusion tracers? JACC Cardiovasc Imaging 2012;5:1269-84.
14. Nekolla SG, Reder S, Saraste A, et al. Evaluation of the novel myocardial perfusion positron-emission tomography tracer 18F-BMS-747158-02: comparison to 13N-ammonia and validation with microspheres in a pig model. Circulation 2009;119:2333-42.
15. El Fakhri G, Sitek A, Guérin B, et al. Quantitative dynamic cardiac 82Rb PET using generalized factor and compartment analyses. J Nucl Med 2005;46:1264-71.
16. Lortie M, Beanlands RS, Yoshinaga K, et al. Quantification of myocardial blood flow with 82Rb dynamic PET imaging. Eur J Nucl Med Mol Imaging 2007;34:1765-74.
17. Efseaff M, Klein R, Ziadi MC, et al. Short-term repeatability of resting myocardial blood flow measurements using rubidium-82 PET imaging. J Nucl Cardiol 2012;19:997-1006.
18. Neglia D, Michelassi C, Trivieri MG, et al. Prognostic role of myocardial blood flow impairment in idiopathic left ventricular dysfunction. Circulation 2002;105:186-93.
19. Shikama N, Himi T, Yoshida K, et al. Prognostic utility of myocardial blood flow assessed by N-13 ammonia positron emission tomography in patients with idiopathic dilated cardiomyopathy. Am J Cardiol 1999;84:434-9.
20. Olivotto I, Cecchi F, Gistri R, et al. Relevance of coronary microvascular flow impairment to long-term remodeling and systolic dysfunction in hypertrophic cardiomyopathy. J Am Coll Cardiol 2006;47:1043-8.
21. Cecchi F, Olivotto I, Gistri R, et al. Coronary microvascular dysfunction and prognosis in hypertrophic cardiomyopathy. N Engl J Med 2003;349:1027-35.
22. Herzog BA, Husmann L, Valenta I, et al. Long-term prognostic value of 13N-ammonia myocardial perfusion positron emission tomography added value of coronary flow reserve. J Am Coll Cardiol 2009;54:150-6.
23. Kajander S, Ukkonen H, Sipilä H, et al. Low radiation dose imaging of myocardial perfusion and coronary angiography with a hybrid PET/CT scanner. Clin Physiol Funct Imaging 2009;29:81-8.
24. Murthy VL, Lee BC, Sitek A, et al. Comparison and prognostic validation of multiple methods of quantification of myocardial blood flow with 82Rb PET. J Nucl Med 2014;55:1952-8.
25. Slomka PJ, Alexanderson E, Jácome R, et al. Comparison of clinical tools for measurements of regional stress and rest myocardial blood flow assessed with 13N-ammonia PET/CT. J Nucl Med 2012;53:171-81.
26. Moody JB, Lee BC, Corbett JR, et al. Precision and accuracy of clinical quantification of myocardial blood flow by dynamic PET: A technical perspective. J Nucl Cardiol 2015;22:935-51.
27. Javadi MS, Lautamäki R, Merrill J, et al. Definition of vascular territories on myocardial perfusion images by integration with true coronary anatomy: a hybrid PET/CT analysis. J Nucl Med 2010;51:198-203.
28. Gaemperli O, Saraste A and Knuuti J. Cardiac hybrid imaging. Eur Heart J Cardiovasc Imaging 2012; 13: 51-60.
29. Ziadi MC, deKemp RA, Beanlands RS. Quantification of Myocardial Perfusion: What will it take to make it to prime time? Curr Cardiovas Imag Rep 2009;2:238-49.
30. Chareonthaitawee P, Kaufmann PA, Rimoldi O, et al. Heterogeneity of resting and hyperemic myocardial blood flow in healthy humans. Cardiovasc Res 2001;50:151-61.
31. Lortie M, Beanlands RS, Yoshinaga K, et al. Quantification of myocardial blood flow with 82Rb dynamic PET imaging. Eur J Nucl Med Mol Imaging 2007;34:1765-74.
32. Uren NG, Camici PG, Melin JA, et al. Effect of aging on myocardial perfusion reserve. J Nucl Med 1995;36:2032-6.
33. Czernin J, Müller P, Chan S, et al. Influence of age and hemodynamics on myocardial blood flow and flow reserve. Circulation 1993;88:62-9.

34. Camici PG, Rimoldi OE. The clinical value of myocardial blood flow measurement. J Nucl Med 2009;50:1076-87.
35. Dayanikli F, Grambow D, Muzik O, et al. Early detection of abnormal coronary flow reserve in asymptomatic men at high risk for coronary artery disease using positron emission tomography. Circulation 1994;90:808-17.
36. Kaufmann PA, Gnecchi-Ruscone T, Di Terlizzi M, et al. Coronary heart disease in smokers: vitamin C restores coronary microcirculatory function. Circulation 2000;102:1233-8.
37. Brush JE, Cannon RO, Schenke WH, et al. Angina due to coronary microvascular disease in hypertensive patients without left ventricular hypertrophy. N Engl J Med 1988;319:1302-7.
38. Geltman EM, Henes CG, Senneff MJ, et al. Increased myocardial perfusion at rest and diminished perfusion reserve in patients with angina and angiographically normal coronary arteries. J Am Coll Cardiol 1990;16:586-95.
39. Johnson BD, Shaw LJ, Buchthal SD, et al. Prognosis in women with myocardial ischemia in the absence of obstructive coronary disease: results from the National Institutes of Health-National Heart, Lung, and Blood Institute-Sponsored Women's Ischemia Syndrome Evaluation (WISE). Circulation 2004;109:2993-9.
40. Gould KL, Lipscomb K, Hamilton GW. Physiologic basis for assessing critical coronary stenosis. Instantaneous flow response and regional distribution during coronary hyperemia as measures of coronary flow reserve. Am J Cardiol 1974;33:87-94.
41. Gould KL. Quantification of coronary artery stenosis in vivo. Circ Res 1985;57:341-53.
42. Uren NG, Melin JA, De Bruyne B, et al. Relation between myocardial blood flow and the severity of coronary-artery stenosis. N Engl J Med 1994;330:1782-8.
43. Beanlands RS, Muzik O, Melon P, et al. Noninvasive quantification of regional myocardial flow reserve in patients with coronary atherosclerosis using nitrogen-13 ammonia positron emission tomography. Determination of extent of altered vascular reactivity. J Am Coll Cardiol 1995;26:1465-75.
44. Di Carli M, Czernin J, Hoh CK, et al. Relation among stenosis severity, myocardial blood flow, and flow reserve in patients with coronary artery disease. Circulation 1995;91:1944-51.
45. Berman DS, Kang X, Slomka PJ, et al. Underestimation of extent of ischemia by gated SPECT myocardial perfusion imaging in patients with left main coronary artery disease. J Nucl Cardiol 2007;14:521-8.
46. Parkash R, Dekemp RA, Ruddy TD, et al. Potential utility of Rubidium 82 PET quantification in patients with 3-vessel coronary artery disease. J Nucl Cardiol 2004;11:440-9.
47. Ziadi MC, Dekemp RA, Williams K, et al. Does quantification of myocardial flow reserve using rubidium-82 positron emission tomography facilitate detection of multivessel coronary artery disease? J Nucl Cardiol 2012;19:670-80.
48. Naya M, Murthy VL, Taqueti VR, et al. Preserved coronary flow reserve effectively excludes high-risk coronary artery disease on angiography. J Nucl Med 2014;55:248-55.
49. Chow BJ, Dennie C, Hoffmann U, et al. Comparison of computed tomographic angiography versus rubidium-82 positron emission tomography for the detection of patients with anatomical coronary artery disease. Can J Cardiol 2007;23:801-7.
50. Valenta I, Dilsizian V, Quercioli A, et al. Quantitative PET/CT measures of myocardial flow reserve and atherosclerosis for cardiac risk assessment and predicting adverse patient outcomes. Curr Cardiol Rep 2013;15:344.
51. Brodov Y, Gransar H, Dey D, et al. Combined quantitative assessment of myocardial perfusion and coronary artery Calcium score by hybrid 82Rb PET/CT improves detection of coronary artery disease. J Nucl Med 2015;56:1345-50.
52. Knaapen P, Germans T, Camici PG, et al. Determinants of coronary microvascular dysfunction in symptomatic hypertrophic cardiomyopathy. Am J Physiol Heart Circ Physiol 2008;294:H986-93.
53. Canetti M, Akhter MW, Lerman A, et al. Evaluation of myocardial blood flow reserve in patients with chronic congestive heart failure due to idiopathic dilated cardiomyopathy. Am J Cardiol 2003;92:1246-9.
54. Ziadi MC, Dekemp RA, Williams KA, et al. Impaired myocardial flow reserve on rubidium-82 positron emission tomography imaging predicts adverse outcomes in patients assessed for myocardial ischemia. J Am Coll Cardiol 2011;58:740-8.
55. Farhad H, Dunet V, Bachelard K, et al. Added prognostic value of myocardial blood flow quantitation in rubidium-82 positron emission tomography imaging. Eur Heart J Cardiovasc Imaging 2013;14:1203-10.
56. Fukushima K, Javadi MS, Higuchi T, et al. Prediction of short-term cardiovascular events using quantification

of global myocardial flow reserve in patients referred for clinical 82Rb PET perfusion imaging. J Nucl Med 2011;52:726-32.
57. Murthy VL, Naya M, Foster CR, et al. Improved cardiac risk assessment with noninvasive measures of coronary flow reserve. Circulation 2011;124:2215-24.
58. Murthy VL, Shah AM, Groarke JD, et al. Coronary vascular dysfunction in the absence of overt coronary atherosclerosis is independently associated with left ventricular diastolic and subclinical systolic dysfunction. Circulation 2012;126:A17175
59. Murthy VL, Naya M, Foster CR, et al. Coronary vascular dysfunction and prognosis in patients with chronic kidney disease. JACC Cardiovasc Imaging 2012;5:1025-34.

Cite this article as: Ziadi MC. Myocardial flow reserve (MFR) with positron emission tomography (PET)/computed tomography (CT): clinical impact in diagnosis and prognosis. Cardiovasc Diagn Ther 2017;7(2):206-218. doi: 10.21037/cdt.2017.04.10

